BIOCHEMISTRY
including biophysical chemistry & molecular biology

Article

pubs.acs.org/biochemistry

Hydrogen/Deuterium Exchange Mass Spectrometry Reveals Specific Changes in the Local Flexibility of Plasminogen Activator Inhibitor 1 upon Binding to the Somatomedin B Domain of Vitronectin

Morten Beck Trelle,[†] Daniel Hirschberg,[†] Anna Jansson,[†] Michael Ploug,[‡] Peter Roepstorff,[†] Peter A. Andreasen,[§] and Thomas J. D. Jørgensen*[,†]

[†]Department of Biochemistry and Molecular Biology, University of Southern Denmark, Campusvej 55, DK-5230 Odense M, Denmark

[‡]Finsen Laboratory, Rigshospitalet and Biotech Research and Innovation Center (BRIC), Copenhagen Biocenter, Jagtvej 124, DK-2200 Copenhagen N, Denmark

[§]Department of Molecular Biology and Genetics, Aarhus University, Gustav Wieds Vej 10, DK-8000 Århus C, Denmark

Supporting Information

ABSTRACT: The native fold of plasminogen activator inhibitor 1 (PAI-1) represents an active metastable conformation that spontaneously converts to an inactive latent form. Binding of the somatomedin B domain (SMB) of the endogenous cofactor vitronectin to PAI-1 delays the transition to the latent state and increases the thermal stability of the protein dramatically. We have used hydrogen/deuterium exchange mass spectrometry to assess the inherent structural flexibility of PAI-1 and to monitor the changes induced by SMB binding. Our data show that the PAI-1 core consisting of β-sheet B is rather protected against exchange with the solvent, while the remainder of the molecule is more dynamic. SMB binding causes a pronounced and widespread stabilization of PAI-1 that is not confined to the binding interface with SMB. We further explored the local structural flexibility in a mutationally stabilized PAI-1 variant (14-1B) as well as the effect of stabilizing antibody Mab-1 on wild-type PAI-1. The three modes of stabilizing PAI-1 (SMB, Mab-1, and the mutations in 14-1B) all cause a delayed latency transition, and this effect was accompanied by unique signatures on the flexibility of PAI-1. Reduced flexibility in the region around helices B, C, and I was seen in all three cases, which suggests an involvement of this region in mediating structural flexibility necessary for the latency transition. These data therefore add considerable depth to our current understanding of the local structural flexibility in PAI-1 and provide novel indications of regions that may affect the functional stability of PAI-1.

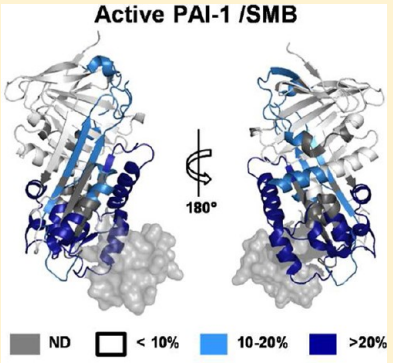

Plasminogen activator inhibitor 1 (PAI-1) is a 379-residue plasma glycoprotein belonging to the serpin superfamily.[1,2] Serpins are highly conserved proteins with a common overall structural fold. Many serpins are inhibitors of serine proteases, and all inhibitory serpins share a common inhibitory mode of action. Serpins are globular proteins (Figure 1) characterized by a solvent-exposed reactive center loop (RCL) that forms the binding site for the target protease. The cleavage of the P1−P1′ bond in the RCL prompts a rapid 70 Å translocation of the protease to the opposite pole of the serpin. During this translocation, the cleaved RCL is inserted as the fourth β-strand in β-sheet A (β4A) and the active site of the protease becomes distorted, preventing completion of the catalytic cycle and release of the protease from the serpin (reviewed in ref 3). Under certain conditions, the protease may dissociate from the RCL prior to insertion of the RCL into β-sheet A, an event termed serpin substrate behavior. The stability of the structural conformations of serpins is usually investigated by thermal denaturation. The active conformation of serpins typically exhibits thermal denaturation in the range between 50 and 60 °C, whereas conformations in which the RCL is inserted in β-sheet A exhibit thermal denaturation points in the 80−120 °C range.[4,5] This difference indicates that the insertion of the RCL into β-sheet A is energetically favorable. The active conformation is therefore often described as the "stressed" conformation relative to the "relaxed" RCL-inserted conformations. The difference in free energy between the stressed and relaxed conformations provides the thermodynamic drive for the conformational change of the serpin and the distortion of the protease during formation of the stable complex. Insertion of the RCL into β-sheet A requires β3A and β5A to slide apart in a shutterlike movement over the underlying hB, and this region of the molecule is thus termed the "shutter region"[6] (Figure 1).

PAI-1 has the ability to spontaneously insert its RCL into β-sheet A, without prior proteolytic cleavage of the RCL, whereby it adopts an inactive "latent" form. For other serpins, adoption of such a latent conformation is a much less facile and rare

Received: July 4, 2012
Revised: September 10, 2012
Published: September 10, 2012

 © 2012 American Chemical Society dx.doi.org/10.1021/bi3008998 | *Biochemistry* 2012, 51, 8256−8266

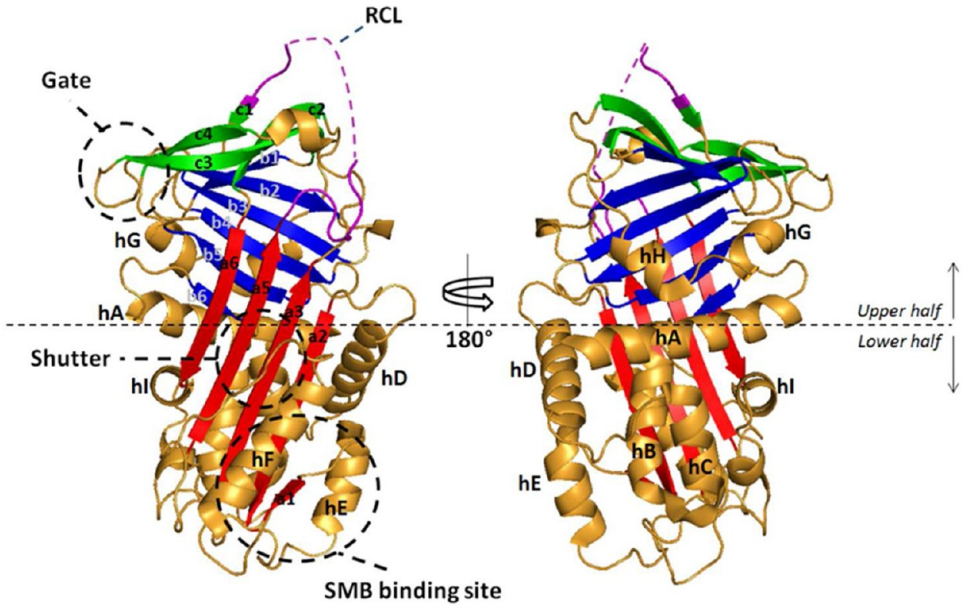

Figure 1. Structure of active PAI-1 (PDB entry 1OC0, 14-1B with SMB bound, SMB not shown) in front (left) and back (right) side views. β-Sheet A is colored red, β-sheet B blue, and β-sheet C green. α-Helices and β-strands are indicated as well as the position of the RCL (magenta, the dotted line indicate lacking residues in the PDB file), the shutter region, the gate region, and the SMB binding interface.

Table 1. Biochemical Properties of Serpins

protein	ligand	protection[a]	effect on latency transition rate[b]	thermal denaturation (°C)
PAI-1				46−52[g]
	vitronectin	nd	1.2−1.4[c]	
	SMB	+++	3[d]	
	Mab-1	+	1.4[e]	
14-1B		++		57−65[h]
	vitronectin	nd	2[f]	
	SMB	+++		ΔT = 20[i]
latent PAI-1		++++		68−70[j]
RCL-cleaved PAI-1			>90[k]	
α1-antitrypsin[n]				~59[l]
neuroserpin[o]				51−56[m]

[a]+, ++, +++, and ++++ indicate increasing levels of overall protection of amide hydrogens against H/D exchange relative to active PAI-1. [b]Values are reported as the x-fold increase in the half-life ($t_{1/2}$) of the latency transition in the presence and absence of ligand. The $t_{1/2}$ for unligated PAI-1 is 1−2 h at 37 °C[10−14] and 12 h at 25 °C,[26] and the $t_{1/2}$ for unligated 14-1B is 145 h at 37 °C.[15] [c]From refs 13 and 14. [d]From ref 24. [e]From ref 13. [f]From ref 47. [g]From refs 15, 16, and 40. [h]From refs 15−17. [i]Increase in thermal denaturation compared to that of unligated 14-1B.[17] [j]From refs 16 and 40. [k]From ref 40. [l]From ref 4. [m]From refs 5 and 41. [n]α1-Antitrypsin does not undergo a latency transition under physiological conditions. [o]Neuroserpin undergoes a latency transition at 45 °C.[5]

process only observed by heating,[7] introduction of certain point mutations,[8,9] or exposure to specific buffer conditions. The kinetics of the PAI-1 latency transition is dependent on numerous factors, including temperature, ionic strength, pH, and the interaction with the endogenous ligand vitronectin.[10−12] Under physiological conditions, the half-life of PAI-1's latency transition is 1−2 h.[10−14] It has proven to be a daunting task to crystallize wild-type PAI-1 in the active conformation for X-ray diffraction. A stabilized tetramutant (N150H/K154T/Q319L/M354I) of PAI-1, termed 14-1B,[15] has therefore been widely used as a model for wild-type PAI-1 in structural studies. Importantly, 14-1B has a dramatically delayed rate of latency transition (half-life of 145 h)[15] and an increased thermal stability (9−13 °C higher, depending on the experiment and technique)[15−17] compared to those of active wild-type PAI-1 (Table 1).

PAI-1 binds vitronectin in its somatomedin B domain (SMB) in a 1:1 stoichiometry with a K_D on the order of 1 nM,[18,19] whereas the affinity for binding of vitronectin to the latent form is at least 200-fold lower.[20] A second PAI-1 binding site with a lower affinity has subsequently been identified in vitronectin.[21,22] The SMB binding interface on the stabilized PAI-1 mutant 14-1B is confined to the area around hE, hF, and β1A (Figure 1), as revealed by X-ray crystallography[17] and site-directed mutagenesis.[23] Binding of vitronectin to active PAI-1 slows the latency transition by approximately 1.4-fold.[13,14] The SMB alone slows the latency transition of wild-type PAI-1 by 3-fold[24] and increases the thermal stability of 14-1B by 20 °C.[17] The exact mechanism by which SMB increases the thermal stability of PAI-1 and delays the latency transition is not clear. The antibody Mab-1 also delays the PAI-1 latency transition to the same extent as vitronectin.[13] Nevertheless, the Mab-1 epitope on PAI-1 is topographically remote from the SMB

dx.doi.org/10.1021/bi3008998 | Biochemistry 2012, 51, 8256−8266

binding site, as it encompass E53 in hC, Q56 in hC, and D305 in the hI–β5A loop.[13] How Mab-1 stabilizes PAI-1 and delays the latency transition is also not known.

It is clear that the biological functions of PAI-1 and the way they are regulated involve conformational plasticity. To understand these complex functions, we therefore need to delineate the inherent structural properties of PAI-1. Hydrogen/deuterium exchange (HDX) mass spectrometry is a powerful technique that can be conveniently used to assess the structural flexibility of proteins in solution. For HDX events to occur on protein backbone amides, they have to be solvent accessible and not engaged in hydrogen bonding. The majority of backbone amides satisfy these criteria only transiently depending on the thermal fluctuations in the molecule. The rate of HDX is therefore a measure of backbone structural flexibility. Using HDX, we now investigate structural flexibility locally in wild-type PAI-1 as well as in stabilized versions thereof, including the physiologically relevant complex with SMB. The HDX results presented here provide considerable insights into the structural flexibility inherent to active PAI-1 and how it is modulated through binding of ligands and introduction of the point mutations in the widely used 14-1B.

MATERIALS AND METHODS

Materials. D_2O (99.9 at. % D) was obtained from Cambridge Isotope Laboratories (Andover, MA), and water was from a Purelab ultra unit (ELGA Labwater). All chemicals were of the highest grade commercially available. Deuterated guanidine HCl was prepared by six repeated cycles of dissolution of guanidine HCl (Sigma-Aldrich, St. Louis, MO) in D_2O and lyophilization. Deuterated PBS buffer (pD 7.8, uncorrected value) was prepared from PBS buffer [0.01 M phosphate buffer, 2.7 mM KCl, and 137 mM NaCl (Sigma-Aldrich PBS tablets)] by two cycles of lyophilization and redissolution in D_2O. Pepsin immobilized on agarose beads was from Pierce (Rockford, IL). Recombinant human active PAI-1 stabilized by four mutations (i.e., N150H, K154T, Q319L, and M354I) and human latent PAI were obtained from Molecular Innovations. Recombinant human active wild-type PAI-1 was produced in *Escherichia coli*. SMB of vitronectin was expressed in *Drosophila melanogaster* S2 cells and purified and characterized as described in ref 25. Protein concentrations were determined by amino acid analysis (Biochrom 30 amino acid analyzer).

Isotopic Exchange. Active wild-type PAI-1, active tetramutant clone 14-1B of PAI-1, and latent PAI-1 were subjected to isotopic exchange of amide hydrogen for deuterium in the presence or absence of a 2-fold molar excess of SMB. Active wild-type PAI-1 was also allowed to undergo isotopic exchange while bound to the PAI-1 clone 1 antibody (Mab-1). All exchange reactions were conducted at 25 °C where the conversion of active PAI-1 to latent PAI-1 is very slow ($t_{1/2}$ = 12 h), and the amount of active PAI-1 converted to latent PAI-1 during the 2 h HDX experiment is therefore negligible.[26] PAI-1 stock solutions with SMB (40 μM PAI-1 and 94 μM SMB) and without SMB (40 μM PAI-1) were prepared and allowed to incubate for 30 min at room temperature. Isotopic exchange was initiated by dilution of 5 μL of PAI-1 or a PAI-1/SMB stock solution into 375 μL of deuterated PBS (pD 7.8, 76-fold dilution) at 25 °C; 75 μL aliquots were taken after 1, 5, 15, 50, and 120 min. Final concentrations of PAI-1 and SMB in the exchange reaction mixture were 0.53 and 1.24 μM, respectively, which is ~500-fold above the K_D for the interaction. Isotopic exchange was immediately quenched by addition of 5 μL of quench solution [8 M guanidine HCl in 10% (v/v) trifluoroacetic acid (TFA)] and snap-frozen in liquid nitrogen, where the samples were stored until further analysis. Isotopic exchange of active wild-type PAI-1 bound to the PAI-1 clone 1 antibody (Mab-1) was done by loading PAI-1 on a column with the immobilized antibody and performing the isotopic exchange on the column. Sepharose beads with immobilized antibody were packed in a 16 μL inner volume Microbore Guard Column (Upchurch Scientific). The column was equilibrated with 200 μL of PBS, loaded with 80 pmol of PAI-1, and washed twice with 200 μL of PBS. The exchange reaction was initiated by passing 100 μL of deuterated PBS through the column and incubating the column for 5 min, 15 min, 50 min, or 2 h at 25 °C. The column was used once for each time point. Wild-type PAI-1 was eluted with 65 μL of elution buffer consisting of a 7.7:1.5:90.8 (v/v) quench solution/water/deuterated PBS mixture. The eluates were snap-frozen in liquid nitrogen, where they were stored until further analysis. A nondeuterated sample was prepared in a similar manner but with dilution in protiated PBS rather than deuterated PBS. To provide a reference point for calculations of deuterium contents relative to the experimental maximum, a fully deuterated PAI-1 control was prepared. This was done by incubation of wild-type PAI-1 in 8 M deuterated guanidine HCl for 4 h at 25 °C.

Desalting and Mass Spectrometric Analysis. The equipment for desalting, online pepsin digestion, and peptide separation has been described previously.[27] In short, solvents were delivered by two Applied Biosystems high-performance liquid chromatography syringe pumps (model 140 B), one for desalting and one for elution of peptides and proteins. Samples were thawed and loaded onto a column (Upchurch Omega Column, 3 mm × 50 mm) packed with immobilized pepsin (Pierce) mounted on a six-port Rheodyne injection valve (7725i). Protein samples were left for 5 min in the pepsin column for digestion and then flushed from the pepsin column to a 10-port, two-position Valco valve (C2-1000A) equipped with a reversed phase C18 microcolumn. The sample was trapped on the microcolumn and desalted with a flow of 0.05% (v/v) TFA for 5 min at a rate of 200 μL/min. For chromatographic separation of peptic peptides, an analytical C18 column (Phenomenex Luna 5u, 2 mm × 150 mm) was mounted in-line with the C18 microcolumn. Peptides were eluted with a 9 min linear gradient from 20 to 100% (v/v) acetonitrile [with 0.05% (v/v) TFA] and analyzed online with a Micromass quadrupole time-of-flight mass spectrometer (QTOF Ultima, Waters, Manchester, U.K.). The spray voltage was set to 3.5 kV, the cone voltage to 55 V, RF lens 1 to 75 V, and the ion source block temperature to 80 °C with a desolvation gas flow of 400 L/h at 200 °C and nebulizing gas flow of 20 L/h at room temperature. To identify peptic peptides, nondeuterated PAI-1 was digested and desalted as described above. The peptic peptides were eluted and collected for nanoflow liquid chromatography (LC)–tandem mass spectrometry (MS/MS) analysis, which was conducted with an Ultimate 3000 nano-liquid chromatograph (Dionex, Sunnyvale, CA) coupled to the mass spectrometer. Data-dependent acquisition was employed to obtain MS/MS spectra of the peptic peptides.

Data Analysis. PAI-1 peptides were identified on the basis of a comparative database search using Mascot (Matrix Science, London, U.K.) on the generated MS/MS spectra. The database

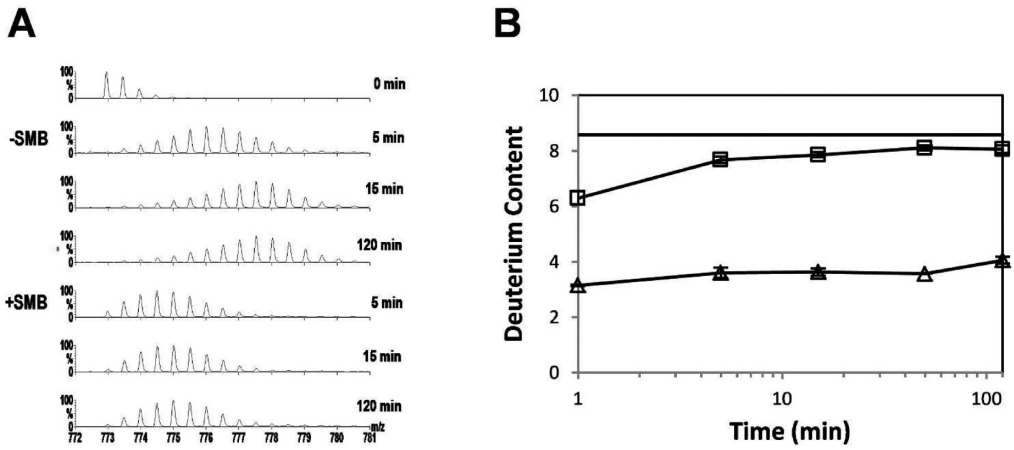

Figure 2. Example data of a deuterium-labeled PAI-1 peptide. Deuterium-labeled PAI-1 was analyzed by LC−MS as described in Materials and Methods. (A) MS spectra of the $(M + 2H)^{2+}$ ion of the peptide 46−59 (m/z 772.91) ion signal after HDX for 5, 15, and 120 min on PAI-1 in the presence and absence of SMB. The 0 min spectrum represents the nondeuterated peptide. (B) Deuterium content plot of peptide 46−59 without (squares) and with (triangles) SMB bound and a full deuteration control indicated by a vertical line. Error bars represent the range between duplicate experiments.

consisted of the human wild-type PAI-1 protein sequence and the tetramutant clone 14-1B protein sequence, and the database was searched with unspecific protease selectivity. The Mascot identifications of peptides were subjected to a manual validation, where the number of assigned fragment ions and their relative intensities and mass accuracies were taken into account. Peptide ion signals were extracted using MassLynx (Waters), smoothed (Savitsky Golay, three times, four-channel smooth window) and centered (four-channel minimum peak width at half-height, 80% centroid top). Peak lists were subsequently exported to Excel (Microsoft, Redmond, WA), and average masses were calculated according to the formula

$$\text{average mass} = \left(\sum_i M_i I_i\right) / \left(\sum_i I_i\right)$$

where i denotes the isotope peak and runs from 1 to the total number of isotopic peaks in the isotopic envelope, M_i denotes the centroid mass of isotope peak i, and I_i denotes the intensity of isotope peak i. Absolute and relative (to full deuteration control) deuterium contents were calculated. For active wild-type PAI-1 with or without SMB and for active wild-type PAI-1 with or without mAb-1, duplicate exchange series were acquired. The average deviation (i.e., half the range between duplicate data points) for all duplicate measurements was 0.14 deuteron, and the relative deviation was 2.1%. The deuterium levels for several peptides changed upon ligand binding, and these changes were typically greater than 15%. A single exchange series was obtained for both latent wild-type PAI-1 with or without SMB and 14-1B with or without SMB.

Peptides covering the mutated amino acids in 14-1B were generally ignored because of the inherent bias in comparing peptides with different amino acid contents. An exception was made for peptide 307−340 because the effect of one residue difference in a 34-amino acid peptide would be relatively small.

RESULTS

Local Flexibility of Active and Latent PAI-1. Isotopic exchange of backbone amide hydrogens with deuterons was initiated by dilution of wild-type PAI-1 into deuterated buffer at 25 °C and pD 7.8. After 1, 5, 15, 50, and 120 min, the exchange reaction was quenched and the protein digested with pepsin. The peptic peptides were subsequently analyzed by LC coupled with MS and deuterium contents calculated and plotted against the exchange time (Figure 2). Deuterium uptake plots for all monitored peptides are included in Figure S1 of the Supporting Information. Relative deuterium contents (i.e., the deuterium uptake relative to the fully deuterated control) for a selection of peptides best representing the sequence are plotted as a heat map along the PAI-1 amino acid sequence (Figure 3).

Consistently, peptides with the lowest relative deuteration levels (32−40, 213−224, 224−235, 352−359, and 360−379) are all located in β-sheet B, and none of them exceeds 60% relative deuteration after exchange for even 120 min (Figures 3 and 4A). This β-sheet is thus the most protected (i.e., least flexible) secondary structural element against HDX in PAI-1. A number of PAI-1 peptides exhibit high relative deuteration levels (>90%) after exchange for just 5 min (Figures 3 and 4A). Peptides representing hD, hE, β1A, and hF (64−92, 99−113, 114−126, and 127−134, respectively) exhibit particularly fast exchange kinetics. This is illustrated by peptide 64−92, covering the entire 12-residue hD, which is almost completely exchanged after 1 min. Helix D thus provides relatively weak structural protection against isotopic exchange in the active conformation of PAI-1. Peptic peptides representing the proximal region of β3A and β5A also exhibit fast exchange kinetics as illustrated by peptide 170−184, which encompasses the three C-terminal residues of β3A and the loop to β4C and is fully exchanged after 5 min (Figure 3). Likewise, peptide 323−339, which comprises the six C-terminal residues of β5A and part of the RCL, contains only a single protected amide hydrogen after exchange for 5 min (Figure S1 of the Supporting Information). The limited protection against HDX observed for the RCL is expected because of the solvent exposure and flexibility of this structure. Nonetheless, residues that are embedded in the proximal parts of β5A and β3A and are contained in these two peptic peptides also populate conformational states, which undergo frequent exchange. This observation highlights a substantial structural flexibility in the apex of β-sheet A.

The local HDX properties of latent PAI-1 were also explored (Figures S2 and S3 of the Supporting Information). Most

dx.doi.org/10.1021/bi3008998 | Biochemistry 2012, 51, 8256−8266

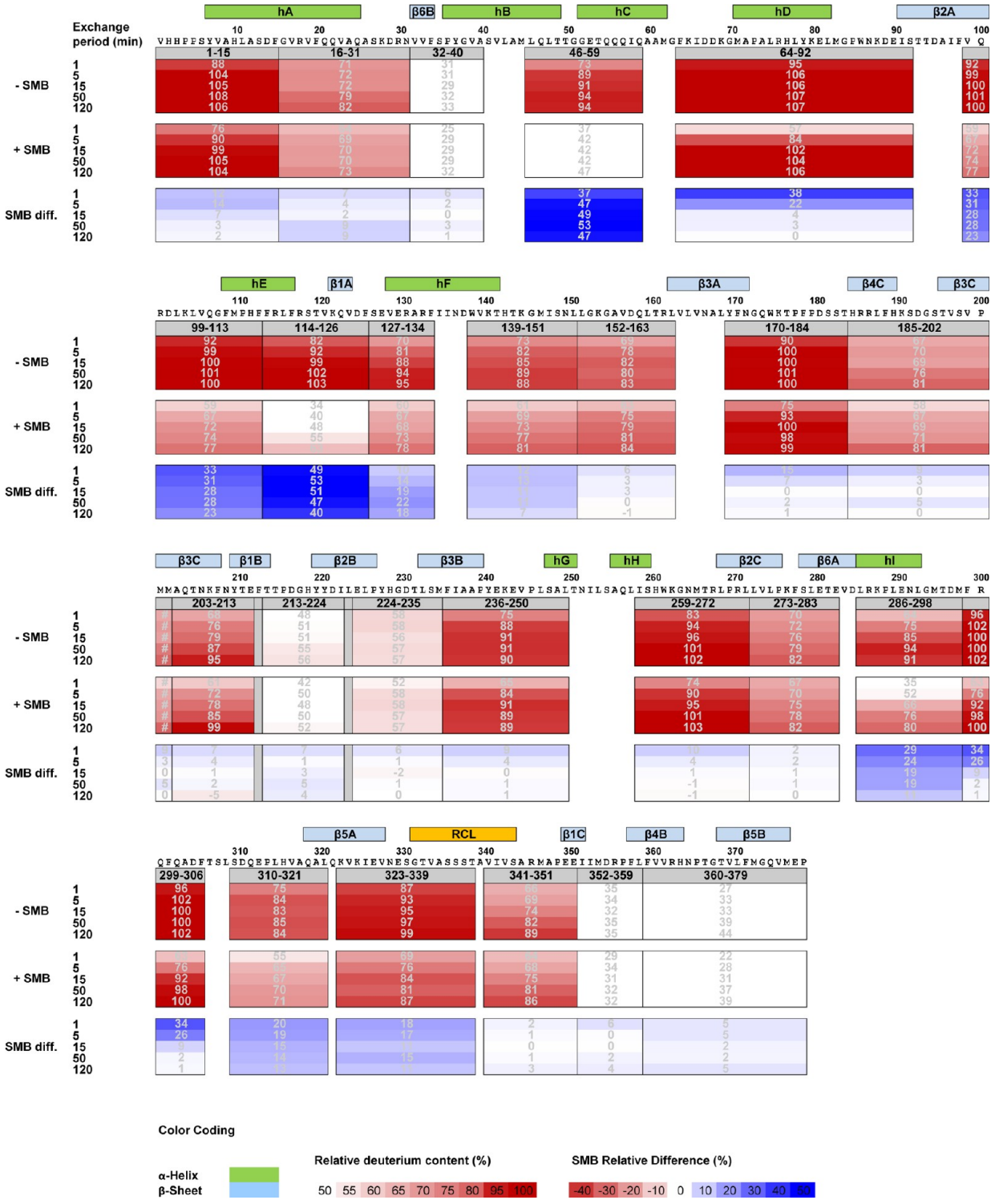

Figure 3. Relative deuterium content in active PAI-1 with and without SMB bound. Heat map representation of relative deuterium contents (in percent) of a select subset of peptides, which provide an optimal sequence coverage for PAI-1. Peptic peptides are represented by gray boxes, and their relative deuterium content is indicated below as a function of exchange time and SMB occupancy. Differential heat maps are shown below the relative deuterium content heat maps, and they are based on the absolute percentage point difference in relative deuterium content with and without SMB bound. Negative (red) values represent faster deuterium incorporation when SMB is bound to PAI-1, and positive (blue) values represent slower deuterium incorporation. α-Helices, β-sheets, and the RCL are indicated above the amino acid sequence.

peptides were more resilient to isotopic exchange in the latent form than in the corresponding active form, with the notable exception of peptide 185−202, which covers β4C and the first C-terminal half of β3C. This peptide was less protected against isotopic exchange in the latent form than in the active form of PAI-1.

Effect of SMB Binding on PAI-1 Flexibility. Next, we investigated the impact of SMB binding on the local flexibility of active PAI-1. This experiment was conducted as described

dx.doi.org/10.1021/bi3008998 | *Biochemistry* 2012, 51, 8256−8266

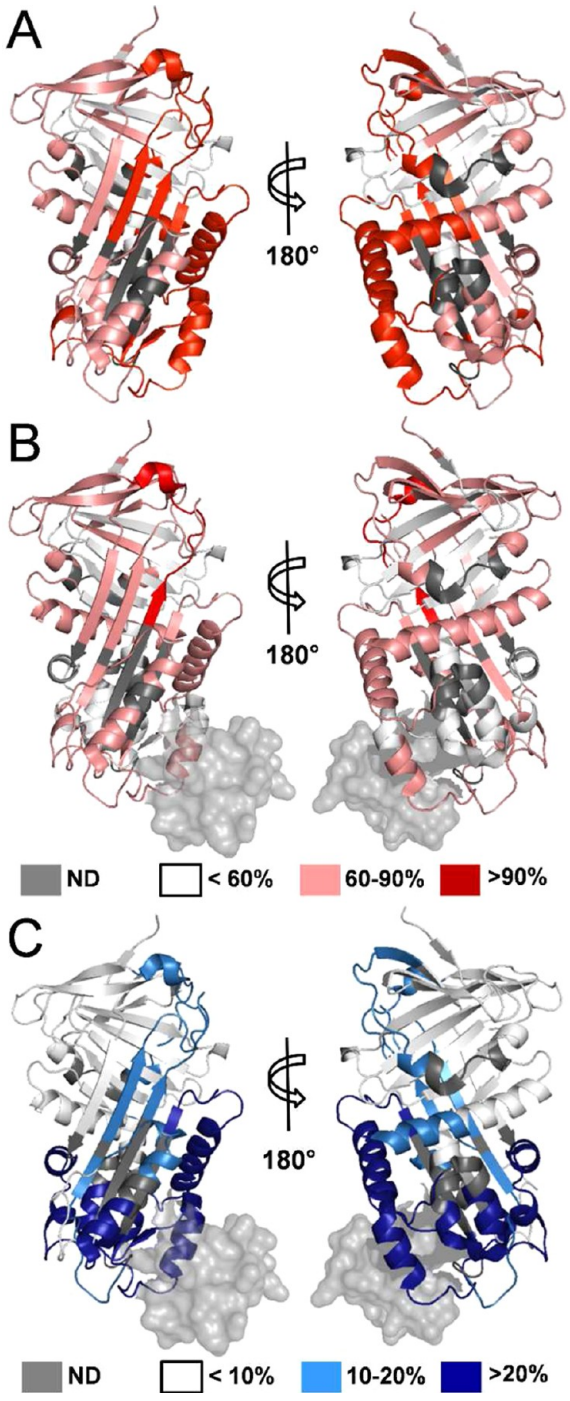

Figure 4. Relative deuterium content of PAI-1 with and without SMB bound mapped on the three-dimensional structure of PAI-1. Relative deuterium content after exchange for 5 min of peptides from Figure 3 mapped on the PAI-1 structure (PDB entry 1OC0, 14-1B with SMB bound) without (A) and with SMB bound (B), according to the indicated color code. (C) Maximal difference in relative deuterium content between PAI-1 with and without SMB bound mapped on the structure of active PAI-1 (PDB entry 1OC0, 14-1B with SMB bound) according to the indicated color code. In panels B and C, the SMB is represented by a gray partially transparent surface.

above but in the presence of a 2-fold molar excess of SMB relative to PAI-1 during the exchange reaction. Deuterium uptake for representative peptic peptides is shown in Figure S1 of the Supporting Information, and the corresponding relative deuterium contents are presented as both a normal and a differential heat map in Figure 3 and mapped on the three-dimensional structure in panels B and C of Figure 4.

SMB binding to PAI-1 induces a widespread and pronounced attenuation of deuterium uptake in PAI-1. Intriguingly, peptides experiencing the strongest protection against isotopic exchange upon SMB occupancy (>10% difference in relative deuterium contents) are generally confined to the lower half of PAI-1. As expected, peptides covering the SMB binding interface[17] (Figure 1) are shielded from the solvent and exhibit particularly slow exchange rates, including peptides 99−113 (β2A−hE), 114−126 (hE−β1A), 127−134 (bottom part of hF), and 139−151 (top part of hF and following loop). However, notable effects were also recorded for peptides remote from the SMB binding site (Figure 4C), including peptides 1−15 (N-terminus of hA), 46−59 (hB and hC), 64−92 (hD), and 286−298, 299−306, and 310−321 (hI and the loop connecting hI with β5A) (Figures 3 and 4C). These peptides are topographically connected in almost a full circle around the vertical axis of the molecule. The only exception is peptide 152−163, which is subjected to weak protection only upon SMB binding (Figure 3). The levels of protection observed in peptides covering hD (64−92), hB and hC (46−59), and hI and the following loop (286−298 with 299−306) are in all cases dramatic, indicating significant conformational stabilization in these structural elements upon SMB binding. Interestingly, protection is also observed in the two peptides (170−184 and 323−339) covering the top of β3A and β5A, when SMB is bound to PAI-1, although this protection is relatively weak for especially peptide 170−184. Peptide 323−339 incorporates ~1 deuteron less throughout the exchange period, and this observation is confirmed by other overlapping peptides [307−340 and 310−321 (Figure S1 of the Supporting Information)]. Whether the protected residues are located in β3A and β5A or in the following loop and RCL cannot be determined. Finally, weak protection against HDX is seen at the earliest time points in a range of peptides covering both β-sheets B and C (Figure 3). However, even shorter exchange times (<1 min) are required to establish the significance and importance of these observations. Taken together, our data show that binding of SMB to active PAI-1 results not only in dramatic stabilization of the actual binding interface but also in almost the entire lower half of the PAI-1 molecule and in a few select areas in the upper half of the molecule.

Effect of Mab-1 Binding on PAI-1 Flexibility. Mab-1 binds to a region on PAI-1 encompassing E53 in hC, Q56 in hC, and D305 in the hI−s5A loop.[13] We investigated the local HDX properties of active wild-type PAI-1 with Mab-1 bound (Figure 5 and Figures S1 and S4 of the Supporting Information) and found a stabilization pattern substantially different from that induced by SMB. In general, the effects of Mab-1 binding appear to be much more focused than those observed when SMB binds. The peptides exhibiting the most predominant protection against HDX are indeed those spanning the proposed binding epitope, i.e., peptides 46−59 (hB and hC) and 286−298 (hI and the following loop) as shown in Figure S1 of the Supporting Information. Only two additional peptides outside the binding epitope are subject to substantial protection, and those are peptides 32−40 (β6B and C-terminal part of hB) and 152−163 (loop following hF). The widespread attenuation of HDX enforced by SMB binding to PAI-1 is thus clearly not recapitulated by Mab-1, although it too prolongs the latency transition.

dx.doi.org/10.1021/bi3008998 | *Biochemistry* 2012, 51, 8256−8266

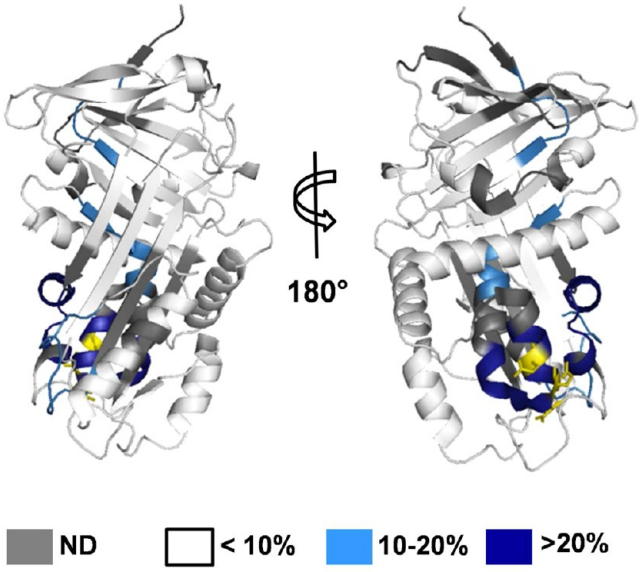

Figure 5. Relative deuterium content differences between wild-type PAI-1 with and without Mab-1 bound mapped on the structure of PAI-1. Maximal difference in relative deuterium content between wild-type PAI-1 with and without Mab-1 bound mapped on the structure of active PAI-1 (PDB entry 1OC0) according to the indicated color scale. PAI-1 residues important for the binding of Mab-1 are colored yellow and shown as sticks.

Local Flexibility of 14-1B. Only moderate protection against HDX was observed in 14-1B when compared to that in wild-type PAI-1 (Figures S1 and S5 of the Supporting Information and Figure 6). Protection was observed in peptides located in the vicinity of the mutated residues. This includes peptide 127−134 (bottom of hF) located in the vicinity of the cluster of N150H, K154T, and Q319L mutations and peptide 273−282 (β2C and β6A) located in the vicinity of the M354I mutation. Other peptides located more remotely from the mutated sites were also protected, such as peptides 32−40 (β6B and top part of hB), 114−126 (top of hE and β1A), 224−235 (β2B and β3B), 286−298 (hI and the following loop), and 46−59 (hB and hC). Peptide 46−59 (hB and hC) was the most protected peptide in 14-1B compared to wild-type PAI-1 (Figure S1 of the Supporting Information). Interestingly, very little protection was observed in peptides spanning β5A and β3A in the shutter region, such as peptides 307−340 and 170−184.

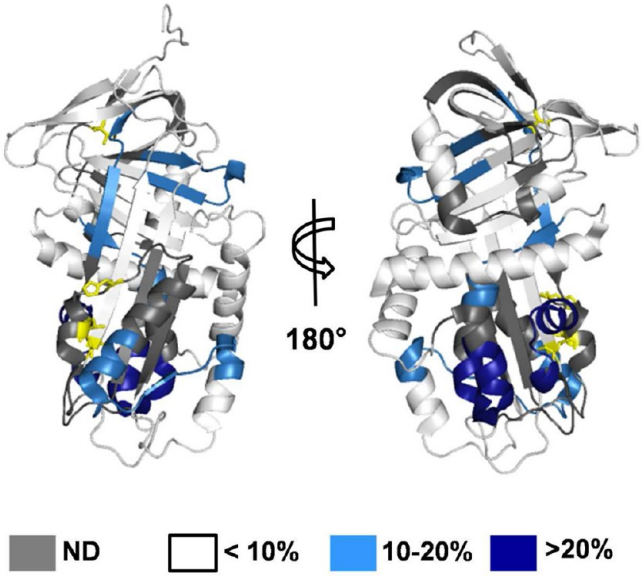

Figure 6. Relative deuterium content differences between wild-type PAI-1 and 14-1B mapped on the structure of PAI-1. Maximal difference in relative deuterium content between wild-type PAI-1 and 14-1B mapped on the structure of 14-1B (PDB entry 1DVM) according to the indicated color code. The mutated residues are colored yellow and shown as sticks.

The effect of binding of SMB to 14-1B was also assessed using HDX, and protection essentially equal to that observed for SMB bound to active wild-type PAI-1 was observed (Figure S1 of the Supporting Information).

DISCUSSION

In this study, we have used HDX to map the structural flexibility of PAI-1 and structural changes induced by the SMB domain of the natural ligand vitronectin, a monoclonal antibody, or a stabilizing set of mutations. We have demonstrated that β-sheet B constitutes a stable core of the protein, whereas other regions are inherently more flexible but become stabilized in a specific manner upon mutagenesis or binding of the somatomedin B domain of vitronectin or monoclonal antibody Mab-1. It is especially noteworthy that there is a clear trend toward stabilization of the otherwise most flexible regions of PAI-1 when it is bound to SMB. In any case, the data provided here clearly show that binding of SMB to PAI-1 serves to maintain PAI-1 in a markedly less flexible conformation, and we provide a topographic map of the affected regions in the protein.

This HDX analysis provides dynamic information that cannot be obtained by X-ray crystal structure analysis. This is clearly exemplified by the fact that overlays of the X-ray structures of PAI-1 (14-1B) with[17] and without SMB bound[28] reveal only small differences in the overall tertiary structure in the lower half of the molecule (Figure S6 of the Supporting Information). It thus appears that the low-energy conformations of PAI-1, which can be monitored by X-ray crystallography, are rather unperturbed by SMB binding. However, our HDX data show substantial protection against HDX when SMB is bound to PAI-1. This protection not only occurs in the SMB binding interface but extends to most of the lower half of the serpin (Figure 4C).

Wintrode and co-workers have previously investigated the local HDX properties of the homologous serpins α_1-antitrypsin[29,30] and neuroserpin[31] under conditions similar to those applied here on PAI-1 (25 °C and pD 7.8). In all three serpins, β-sheet B and partly β-sheet C were the structures most protected against HDX, suggesting a conserved stability in this region of serpins. Similarly, the N-terminal part of hA, hD, and the RCL were among the most flexible regions in all three serpins[29,31] (Figures 3 and 4A). β3A and β5A were relatively protected against HDX in α_1-antitrypsin,[29] whereas residues embedded in these two strands were relatively unprotected in both neuroserpin[31] and PAI-1 (Figures 3 and 4A). Similarly, the N-terminal part of hC appears to be less protected against HDX in PAI-1 and neuroserpin[31] than in α1-antitrypsin.[29] The question of whether these differences are related to the different functional properties of the three serpins remains unknown. PAI-1 was also investigated previously using HDX, but

dx.doi.org/10.1021/bi3008998 | *Biochemistry* 2012, 51, 8256−8266

inconsistencies in the reported data[32] render a comparison with the results reported here problematic.

Structural Dynamics of PAI-1 in Solution. The local HDX analysis of PAI-1 revealed a slowly exchanging core, composed primarily of β-sheet B, and a relatively faster exchanging remainder of the molecule (Figure 4). Especially peptides covering hD, hE, β1A, and hF displayed very little protection against HDX. Structural flexibility in these areas of PAI-1 has previously been indicated by limited proteolysis,[33] but the data reported here indicate additional areas of high structural flexibility, including the N-terminal half of hA, the loop between β3A and β4C, and part of the loop between hI and β5A (Figures 3 and 4A). HDX data obtained for the latent form of PAI-1 provide direct evidence that the stabilization gained upon the transition to the latent state is nearly global. In agreement with data obtained by limited proteolysis,[33] the peptide spanning β4C, the following loop, and part of β3C (residues 185−202) was in the present study found to be more flexible in the latent form than in the active form, indicating that dislocation of the RCL and β1C from β-sheet C destabilizes this region.

SMB Induces Widespread Structural Stabilization in PAI-1. Apart from a dramatic stabilization of most of the lower half of PAI-1, SMB also stabilizes a few areas in the upper half of the molecule. It has previously been shown that binding of vitronectin to PAI-1 has an effect on the conformation of the reactive center loop[34,35] and the specificity toward target proteases in a PAI-1 mutant.[36] A change in the flexibility of peptides covering the RCL when SMB is bound to PAI-1 would thus support these observations. In fact, peptide 323−339, which spans the C-terminal half of β5A and the N-terminal half of the RCL, is more protected against HDX when SMB is bound (Figure 3). However, from the data reported here, we cannot determine which residues are subject to the protection in the peptide, and it could be only the residues of β5A. Interestingly, we observe no significant change in the HDX properties of peptide 341−351, containing the scissile P1−P1′ bond (R346−M347). Thus, SMB binding does not appear to affect the structural flexibility of this region. It should be noted, however, that a change in the flexibility of the loop that is not accompanied by any protection of its amide hydrogens would be resilient to detection by HDX.

How Do Induced Changes in the HDX Properties of PAI-1 Correlate with the Functional Stability? Binding of either vitronectin or Mab-1 to active PAI-1 slows the latency transition by approximately 1.4-fold[13,14] and provides stabilization against substrate behavior and polymerization,[13,37] whereas the mutations in 14-1B slow the latency transition by approximately 100-fold. From the induced changes in HDX properties measured here, we can gain insight into the local dynamic properties of PAI-1, governing its functional stability.

The functional importance of the region around helices B, C, and I is not known apart from binding of the Mab-1 antibody and the effects that this interaction has on the biochemical properties of PAI-1.[13,38] It is therefore both interesting and intriguing that peptides covering this region [residues 46−59 and 286−298 (Figure S1 of the Supporting Information)] are dramatically stabilized in all experiments (PAI-1 with or without SMB, PAI-1 with or without Mab-1 and 14-1B) where latency transition is known to be delayed. The impact on hB, hC, and hI when PAI-1 is bound to SMB and in 14-1B is especially intriguing. The mutated residues in 14-1B and the SMB binding interface with PAI-1 are not in the immediate vicinity of these helices, and the observed stabilizations thus imply allostery in the structural flexibility of the lower part of PAI-1. What role the flexibility of hB, hC, and hI plays in the mechanism of latency transition, or even global stability, is not clear. Structural flexibility in this region may act as a point of origin for structural flexibility elsewhere in the molecule and thereby be linked to a transition state in the process of latency transition. While such a mechanism may be valid for wild-type PAI-1, it is, however, probably not the major reason for the delayed latency transition in 14-1B. The stabilization of hB and hC (peptide 46−59) in 14-1B is not as strong as in wild-type PAI-1 with SMB and Mab-1 bound, despite 14-1B exhibiting the most delayed latency transition.

In 14-1B, three of the four mutations (N150H, K154T, and Q319L) are located in the interaction surface between the hF−β3A loop and the bottom half of β-sheet A, and they, on their own, delayed the latency transition half-life to 36.3 h.[15] Nonetheless, no significant stabilization of peptides covering β3A and β5A [170−184 and 307−340 (Figure S1 of the Supporting Information)] was observed in 14-1B. Likewise, no protection was observed in these peptides when Mab-1 was bound to wild-type PAI-1. This clearly indicates that latency transition can be delayed without the reduction of flexibility in the C-terminal residues of β3A and β5A. This is noteworthy considering the very high flexibility of these residues in wild-type unligated PAI-1 (Figure 3). In the case of 14-1B, we were unable to obtain HDX data from an area around the N150H/K154T/Q319L cluster of mutations. Although speculative, it is possible that this region is stabilized in 14-1B and thereby affects the rate of insertion of the uncleaved RCL in the lower half of β-sheet A. Protection was also observed in peptide 273−283, covering β6A and part of β2C, which make direct contact with the M354I mutation. This mutation alone reduces the latency transition half-life to 6.6 h,[15] possibly through enhanced tethering of β1C to β-sheet C. Such a mechanism is in agreement with the protection against HDX observed in peptide 273−283.

Finally, weak protection against HDX was observed in peptide 32−40 covering all of β6B and the six N-terminal residues of hB in both 14-1B and Mab-1 bound to wild-type PAI-1 (Figure S1 of the Supporting Information). This peptide is located in the hydrophobic core of the structure, sandwiched between β-sheet A and helix A, and contains residues involved in the hydrogen bonding network of the shutter region.[28,39] A stabilization of this region may affect the accessibility of β-sheet A for insertion of the RCL during latency transition but it would have to do so without a significant decrease in the flexibility of the C-terminal residues of β3A and β5A because no protection was observed there. In any case, it is noteworthy that a peptide that is situated in the hydrophobic core of the protein and is among the most protected peptides against HDX in the active form of PAI-1 becomes even further protected under circumstances associated with a delay in the latency transition. Although the changes in HDX properties are small in peptide 32−40, it is directly connected to the hB−hC region that is substantially stabilized in 14-1B and when Mab-1 is bound to wild-type PAI-1. This suggests cross-talk between flexibility in hB and hC and further up and into the core of the protein. Interestingly, when SMB was bound to PAI-1, no significant protection was seen in peptide 32−40, but instead, a number of peptides covering β-sheets B and C displayed reduced levels of deuterium incorporation at the very earliest time points (Figure 3).

dx.doi.org/10.1021/bi3008998 | Biochemistry 2012, 51, 8256−8266

Is There a Correlation between Thermodynamic Stability and the Rate of the Latency Transition in PAI-1? The metastability of PAI-1 in its active conformation, as compared to other serpins, is evident from a low thermal stability (T_m = 46−52 °C)[15,16,40] and an ability to spontaneously convert to the latent form under physiological conditions (Table 1). Active α_1-antitrypsin has a melting point of ∼59 °C[4] and does not convert to the latent form under physiological conditions. Neuroserpin, on the other hand, has a melting point around 51−56 °C[5,41] and also converts to the latent form under physiological conditions but with a half-life of >24 h.[42] A correlation between protein stability and inhibitory activity was previously shown in α_1-antitrypsin mutants.[43,44] On the basis of these data, it was suggested that the process of protease inhibition and the process of unfolding in low concentrations of guanidine required a population of a shared molten globule intermediate.[43] This notion implies an intersection between the energy landscape of folding and unfolding and the functional energy landscape in α_1-antitrypsin. As judged by thermal denaturation, there is no simple correlation between the global stability of PAI-1 and the rate of latency transition, and this notion is supported by the HDX properties reported here (Table 1). The overall protection against HDX, in each of the experiments conducted, was assessed semiquantitatively and taken as a measure of overall structural flexibility. Clearly, in experiments where the thermal denaturation point is elevated in PAI-1 (with SMB bound to wild-type PAI-1 and in 14-1B), we also observe protection against HDX (Table 1). However, there was no simple correlation between overall protection against HDX and the rate of latency transition. Binding of SMB to wild-type PAI-1 induces substantial protection against HDX, but an only 3-fold increase in the half-life of latency transition. The mutations in 14-1B, on the other hand, cause only moderate protection against HDX but a much stronger retardation of latency transition. The significant retardation of latency transition in 14-1B is therefore unlikely to be a result of a lowered thermodynamic drive toward the latent conformation but rather through the existence of significant activation energy barriers that are not present in wild-type PAI-1. This supports the view that 14-1B has limitations in its applicability as a model for wild-type PAI-1, especially with respect to the dynamic properties of the molecule. Recently, the X-ray crystal structure of another PAI-1 variant with a W175F mutation was determined, and the mutant was shown to have normal thermal stability but a 3-fold delayed latency transition.[16] Not only is this mutant a more applicable model for wild-type PAI-1 given its normal thermal stability, but it also provides another example of the lack of correlation between thermodynamic stability and the rate of latency transition in PAI-1.

What Is the Function of the PAI-1−Vitronectin Interaction? Vitronectin plays important roles in the regulation of hemostasis and cell adhesion through interactions with heparin, PAI-1, integrins $\alpha_v\beta_1$ and $\alpha_v\beta_5$, and the urokinase-type plasminogen activator receptor (uPAR). The binding of vitronectin to PAI-1 is thought to attenuate fibrinolysis through localization of PAI-1 in the vicinity of clots[45] and in the extracellular matrix,[46] but as shown here by HDX, vitronectin induces widespread conformational changes in PAI-1. Exactly how vitronectin stabilizes PAI-1 is not completely understood, but the dramatic increase in the melting point of 14-1B upon binding to SMB[17] indicates a significant stabilization of interactions important for the maintenance of the overall fold of the protein. Is the functional stabilization of PAI-1 by vitronectin physiologically relevant? Although this is still unclear, it is difficult to imagine that the nanomolar affinity between vitronectin and PAI-1 and the widespread vitronectin-induced structural changes in PAI-1 have evolved to cause a mere 2-fold, or smaller, delay in latency transition. Perhaps the main function of the PAI-1−vitronectin interaction is just a matter of PAI-1 localization and the conformational changes were coincidental or necessary traits that came with the evolution of the high binding affinity, or maybe some functions of the interaction still elude us.

■ CONCLUSION

In conclusion, the HDX-based investigation of PAI-1 reported here provides novel insight into the spatial distribution of relatively flexible and inflexible regions in the molecule and how local flexibility is modulated upon binding of the SMB domain of vitronectin. It is well-known that vitronectin binds PAI-1 with high affinity and conveys functional stability to the serpin, but the mechanistic details of this effect remain elusive. However, the data reported here clearly show that binding of the SMB domain to PAI-1 causes dramatic and widespread stabilization in most of the lower half of the serpin. Furthermore, the consistent protection against deuterium incorporation in helices B, C, and I under experimental conditions where PAI-1 latency transition is delayed suggests a role for this region in mediating the structural flexibility necessary for the process of latency transition.

■ ASSOCIATED CONTENT

Supporting Information

Deuterium content plots of all analyzed peptides (Figure S1), relative deuterium content map of active wild-type PAI-1 versus latent wild-type PAI-1 (Figure S2), relative deuterium content differences between wild-type PAI-1 in the active and latent conformations mapped on the structure of latent PAI-1 (Figure S3), relative deuterium content map of active PAI-1 with and without Mab-1 bound (Figure S4), relative deuterium content map of active wild-type PAI-1 versus active tetramutant 14-1B (Figure S5), and overlays of the X-ray structures of PAI-1 with and without SMB bound (Figure S6). This material is available free of charge via the Internet at http://pubs.acs.org.

■ AUTHOR INFORMATION

Corresponding Author

*Department of Biochemistry and Molecular Biology, University of Southern Denmark, DK-5230 Odense M, Denmark. Telephone: +45-6550 2409. Fax: +45-6550 2467. E-mail: tjdj@bmb.sdu.dk.

Author Contributions

M.B.T. and D.H. contributed equally to this work.

Funding

M.B.T., P.A.A., and T.J.D.J. were supported by a grant from the Danish Research Council for Technical Sciences and Production (09-072885). D.H. was supported by a grant from the Villum Kann Rasmussen Foundation. A.J. was supported by an EMBO fellowship.

Notes

The authors declare no competing financial interest.

■ ACKNOWLEDGMENTS

We thank Hua Zhang (University of Southern Denmark) for excellent technical assistance and Jeppe B. Madsen and Dr. Jan K. Jensen (Aarhus University) for valuable scientific advice and comments.

■ ABBREVIATIONS

PAI-1, plasminogen activator inhibitor 1; SMB, somatomedin B domain; HDX, hydrogen−deuterium exchange; RCL, reactive center loop; PDB, Protein Data Bank; uPAR, urokinase-type plasminogen activator receptor.

■ REFERENCES

(1) Gettins, P. G. (2002) Serpin structure, mechanism, and function. *Chem. Rev. 102*, 4751−4804.
(2) Dupont, D. M., Madsen, J. B., Kristensen, T., Bodker, J. S., Blouse, G. E., Wind, T., and Andreasen, P. A. (2009) Biochemical properties of plasminogen activator inhibitor-1. *Front. Biosci. 14*, 1337−1361.
(3) Wind, T., Hansen, M., Jensen, J. K., and Andreasen, P. A. (2002) The molecular basis for anti-proteolytic and non-proteolytic functions of plasminogen activator inhibitor type-1: Roles of the reactive centre loop, the shutter region, the flexible joint region and the small serpin fragment. *Biol. Chem. 383*, 21−36.
(4) Kaslik, G., Kardos, J., Szabo, E., Szilagyi, L., Zavodszky, P., Westler, W. M., Markley, J. L., and Graf, L. (1997) Effects of serpin binding on the target proteinase: global stabilization, localized increased structural flexibility, and conserved hydrogen bonding at the active site. *Biochemistry 36*, 5455−5464.
(5) Takehara, S., Onda, M., Zhang, J., Nishiyama, M., Yang, X., Mikami, B., and Lomas, D. A. (2009) The 2.1-Å crystal structure of native neuroserpin reveals unique structural elements that contribute to conformational instability. *J. Mol. Biol. 388*, 11−20.
(6) Stein, P., and Chothia, C. (1991) Serpin tertiary structure transformation. *J. Mol. Biol. 221*, 615−621.
(7) Carrell, R. W., Stein, P. E., Fermi, G., and Wardell, M. R. (1994) Biological implications of a 3 Å structure of dimeric antithrombin. *Structure 2*, 257−270.
(8) Beauchamp, N. J., Pike, R. N., Daly, M., Butler, L., Makris, M., Dafforn, T. R., Zhou, A., Fitton, H. L., Preston, F. E., Peake, I. R., and Carrell, R. W. (1998) Antithrombins Wibble and Wobble (T85M/K): Archetypal conformational diseases with in vivo latent-transition, thrombosis, and heparin activation. *Blood 92*, 2696−2706.
(9) Im, H., Woo, M. S., Hwang, K. Y., and Yu, M. H. (2002) Interactions causing the kinetic trap in serpin protein folding. *J. Biol. Chem. 277*, 46347−46354.
(10) Lindahl, T. L., Sigurdardottir, O., and Wiman, B. (1989) Stability of plasminogen activator inhibitor 1 (PAI-1). *Thromb. Haemostasis 62*, 748−751.
(11) Sancho, E., Tonge, D. W., Hockney, R. C., and Booth, N. A. (1994) Purification and characterization of active and stable recombinant plasminogen-activator inhibitor accumulated at high levels in *Escherichia coli*. *Eur. J. Biochem. 224*, 125−134.
(12) Declerck, P. J., De Mol, M., Alessi, M. C., Baudner, S., Paques, E. P., Preissner, K. T., Muller-Berghaus, G., and Collen, D. (1988) Purification and characterization of a plasminogen activator inhibitor 1 binding protein from human plasma. Identification as a multimeric form of S protein (vitronectin). *J. Biol. Chem. 263*, 15454−15461.
(13) Bodker, J. S., Wind, T., Jensen, J. K., Hansen, M., Pedersen, K. E., and Andreasen, P. A. (2003) Mapping of the epitope of a monoclonal antibody protecting plasminogen activator inhibitor-1 against inactivating agents. *Eur. J. Biochem. 270*, 1672−1679.
(14) Hansen, M., Busse, M. N., and Andreasen, P. A. (2001) Importance of the amino-acid composition of the shutter region of plasminogen activator inhibitor-1 for its transitions to latent and substrate forms. *Eur. J. Biochem. 268*, 6274−6283.
(15) Berkenpas, M. B., Lawrence, D. A., and Ginsburg, D. (1995) Molecular evolution of plasminogen activator inhibitor-1 functional stability. *EMBO J. 14*, 2969−2977.
(16) Jensen, J. K., Thompson, L. C., Bucci, J. C., Nissen, P., Gettins, P. G., Peterson, C. B., Andreasen, P. A., and Morth, J. P. (2011) Crystal structure of plasminogen activator inhibitor-1 in an active conformation with normal thermodynamic stability. *J. Biol. Chem. 286*, 29709−29717.
(17) Zhou, A., Huntington, J. A., Pannu, N. S., Carrell, R. W., and Read, R. J. (2003) How vitronectin binds PAI-1 to modulate fibrinolysis and cell migration. *Nat. Struct. Biol. 10*, 541−544.
(18) Salonen, E. M., Vaheri, A., Pollanen, J., Stephens, R., Andreasen, P., Mayer, M., Dano, K., Gailit, J., and Ruoslahti, E. (1989) Interaction of plasminogen activator inhibitor (PAI-1) with vitronectin. *J. Biol. Chem. 264*, 6339−6343.
(19) Seiffert, D., and Loskutoff, D. J. (1991) Kinetic analysis of the interaction between type 1 plasminogen activator inhibitor and vitronectin and evidence that the bovine inhibitor binds to a thrombin-derived amino-terminal fragment of bovine vitronectin. *Biochim. Biophys. Acta 1078*, 23−30.
(20) Lawrence, D. A., Palaniappan, S., Stefansson, S., Olson, S. T., Francis-Chmura, A. M., Shore, J. D., and Ginsburg, D. (1997) Characterization of the binding of different conformational forms of plasminogen activator inhibitor-1 to vitronectin. Implications for the regulation of pericellular proteolysis. *J. Biol. Chem. 272*, 7676−7680.
(21) Schar, C. R., Jensen, J. K., Christensen, A., Blouse, G. E., Andreasen, P. A., and Peterson, C. B. (2008) Characterization of a site on PAI-1 that binds to vitronectin outside of the somatomedin B domain. *J. Biol. Chem. 283*, 28487−28496.
(22) Schar, C. R., Blouse, G. E., Minor, K. H., and Peterson, C. B. (2008) A deletion mutant of vitronectin lacking the somatomedin B domain exhibits residual plasminogen activator inhibitor-1-binding activity. *J. Biol. Chem. 283*, 10297−10309.
(23) Jensen, J. K., Wind, T., and Andreasen, P. A. (2002) The vitronectin binding area of plasminogen activator inhibitor-1, mapped by mutagenesis and protection against an inactivating organochemical ligand. *FEBS Lett. 521*, 91−94.
(24) Seiffert, D., Ciambrone, G., Wagner, N. V., Binder, B. R., and Loskutoff, D. J. (1994) The somatomedin B domain of vitronectin. Structural requirements for the binding and stabilization of active type 1 plasminogen activator inhibitor. *J. Biol. Chem. 269*, 2659−2666.
(25) Kjaergaard, M., Gardsvoll, H., Hirschberg, D., Nielbo, S., Mayasundari, A., Peterson, C. B., Jansson, A., Jorgensen, T. J., Poulsen, F. M., and Ploug, M. (2007) Solution structure of recombinant somatomedin B domain from vitronectin produced in *Pichia pastoris*. *Protein Sci. 16*, 1934−1945.
(26) Mathiasen, L., Dupont, D. M., Christensen, A., Blouse, G. E., Jensen, J. K., Gils, A., Declerck, P. J., Wind, T., and Andreasen, P. A. (2008) A peptide accelerating the conversion of plasminogen activator inhibitor-1 to an inactive latent state. *Mol. Pharmacol. 74*, 641−653.
(27) Rist, W., Mayer, M. P., Andersen, J. S., Roepstorff, P., and Jorgensen, T. J. (2005) Rapid desalting of protein samples for on-line microflow electrospray ionization mass spectrometry. *Anal. Biochem. 342*, 160−162.
(28) Stout, T. J., Graham, H., Buckley, D. I., and Matthews, D. J. (2000) Structures of active and latent PAI-1: A possible stabilizing role for chloride ions. *Biochemistry 39*, 8460−8469.
(29) Tsutsui, Y., Liu, L., Gershenson, A., and Wintrode, P. L. (2006) The conformational dynamics of a metastable serpin studied by hydrogen exchange and mass spectrometry. *Biochemistry 45*, 6561−6569.
(30) Sengupta, T., Tsutsui, Y., and Wintrode, P. L. (2009) Local and global effects of a cavity filling mutation in a metastable serpin. *Biochemistry 48*, 8233−8240.
(31) Sarkar, A., Zhou, C., Meklemburg, R., and Wintrode, P. L. (2011) Local conformational flexibility provides a basis for facile polymer formation in human neuroserpin. *Biophys. J. 101*, 1758−1765.
(32) Nukuna, B. N., Penn, M. S., Anderson, V. E., and Hazen, S. L. (2004) Latency and substrate binding globally reduce solvent

accessibility of plasminogen activator inhibitor type 1 (PAI-1). An adaptation of PAI-1 conformer crystal structures by hydrogen-deuterium exchange. *J. Biol. Chem. 279*, 50132−50141.
(33) Egelund, R., Schousboe, S. L., Sottrup-Jensen, L., Rodenburg, K. W., and Andreasen, P. A. (1997) Type-1 plasminogen-activator inhibitor: Conformational differences between latent, active, reactive-centre-cleaved and plasminogen-activator-complexed forms, as probed by proteolytic susceptibility. *Eur. J. Biochem. 248*, 775−785.
(34) Fa, M., Karolin, J., Aleshkov, S., Strandberg, L., Johansson, L. B., and Ny, T. (1995) Time-resolved polarized fluorescence spectroscopy studies of plasminogen activator inhibitor type 1: Conformational changes of the reactive center upon interactions with target proteases, vitronectin and heparin. *Biochemistry 34*, 13833−13840.
(35) Gibson, A., Baburaj, K., Day, D. E., Verhamme, I., Shore, J. D., and Peterson, C. B. (1997) The use of fluorescent probes to characterize conformational changes in the interaction between vitronectin and plasminogen activator inhibitor-1. *J. Biol. Chem. 272*, 5112−5121.
(36) Keijer, J., Ehrlich, H. J., Linders, M., Preissner, K. T., and Pannekoek, H. (1991) Vitronectin governs the interaction between plasminogen activator inhibitor 1 and tissue-type plasminogen activator. *J. Biol. Chem. 266*, 10700−10707.
(37) Egelund, R., Einholm, A. P., Pedersen, K. E., Nielsen, R. W., Christensen, A., Deinum, J., and Andreasen, P. A. (2001) A regulatory hydrophobic area in the flexible joint region of plasminogen activator inhibitor-1, defined with fluorescent activity-neutralizing ligands. Ligand-induced serpin polymerization. *J. Biol. Chem. 276*, 13077−13086.
(38) Kjoller, L., Martensen, P. M., Sottrup-Jensen, L., Justesen, J., Rodenburg, K. W., and Andreasen, P. A. (1996) Conformational changes of the reactive-centre loop and β-strand 5A accompany temperature-dependent inhibitor-substrate transition of plasminogen-activator inhibitor 1. *Eur. J. Biochem. 241*, 38−46.
(39) Harrop, S. J., Jankova, L., Coles, M., Jardine, D., Whittaker, J. S., Gould, A. R., Meister, A., King, G. C., Mabbutt, B. C., and Curmi, P. M. (1999) The crystal structure of plasminogen activator inhibitor 2 at 2.0 Å resolution: Implications for serpin function. *Structure 7*, 43−54.
(40) Lawrence, D. A., Olson, S. T., Palaniappan, S., and Ginsburg, D. (1994) Serpin reactive center loop mobility is required for inhibitor function but not for enzyme recognition. *J. Biol. Chem. 269*, 27657−27662.
(41) Belorgey, D., Crowther, D. C., Mahadeva, R., and Lomas, D. A. (2002) Mutant neuroserpin (S49P) that causes familial encephalopathy with neuroserpin inclusion bodies is a poor proteinase inhibitor and readily forms polymers in vitro. *J. Biol. Chem. 277*, 17367−17373.
(42) Onda, M., Belorgey, D., Sharp, L. K., and Lomas, D. A. (2005) Latent S49P neuroserpin forms polymers in the dementia familial encephalopathy with neuroserpin inclusion bodies. *J. Biol. Chem. 280*, 13735−13741.
(43) Tsutsui, Y., and Wintrode, P. L. (2007) Cooperative unfolding of a metastable serpin to a molten globule suggests a link between functional and folding energy landscapes. *J. Mol. Biol. 371*, 245−255.
(44) Seo, E. J., Lee, C., and Yu, M. H. (2002) Concerted regulation of inhibitory activity of α1-antitrypsin by the native strain distributed throughout the molecule. *J. Biol. Chem. 277*, 14216−14220.
(45) Podor, T. J., Campbell, S., Chindemi, P., Foulon, D. M., Farrell, D. H., Walton, P. D., Weitz, J. I., and Peterson, C. B. (2002) Incorporation of vitronectin into fibrin clots. Evidence for a binding interaction between vitronectin and γA/γ' fibrinogen. *J. Biol. Chem. 277*, 7520−7528.
(46) Pollanen, J., Saksela, O., Salonen, E. M., Andreasen, P., Nielsen, L., Dano, K., and Vaheri, A. (1987) Distinct localizations of urokinase-type plasminogen activator and its type 1 inhibitor under cultured human fibroblasts and sarcoma cells. *J. Cell Biol. 104*, 1085−1096.
(47) Li, S. H., Gorlatova, N. V., Lawrence, D. A., and Schwartz, B. S. (2008) Structural differences between active forms of plasminogen activator inhibitor type 1 revealed by conformationally sensitive ligands. *J. Biol. Chem. 283*, 18147−18157.